Research Highlights

- Pseudo–simultaneous measurements at all 4 seats in car, and inside–outside taken
- Identical PNCs at all 4 seats indicated car cabin air is well–mixed
- Ratio of in–cabin to outside PNCs is not uniform for different particle sizes
- Time scale analysis highlights dilution as a dominating process
- A proposed semi–empirical model predicted inside cabin PNC adequately well

Citation details:
Joodatnia, P., Kumar, P., Robins, A., 2013. Fast response sequential measurements and modelling of nanoparticles inside and outside a car cabin. Atmospheric Environment 71, 364-375. http://dx.doi.org/10.1016/j.atmosenv.2013.02.028

Fast response sequential measurements and modelling of nanoparticles inside and outside a car cabin

Pouyan Joodatnia [a], Prashant Kumar [a, b, 1], Alan Robins [b]

[a]*Department of Civil and Environmental Engineering, Faculty of Engineering and Physical Science (FEPS), University of Surrey, GU2 7XH, United Kingdom*

[b]*Environmental Flow (EnFlo) Research Centre, FEPS, University of Surrey, GU2 7XH, United Kingdom*

Abstract

Commuters are regularly exposed to short-term peak concentration of traffic produced nanoparticles (i.e. particles <300 nm in size). Studies indicate that these exposures pose adverse health effects (i.e. cardiovascular). This study aims to obtain particle number concentrations (PNCs) and distributions (PNDs) inside and outside a car cabin whilst driving on a road in Guildford, a typical UK town. Other objectives are to: (i) investigate the influences of particle transformation processes on particle number and size distributions in the cabin, (ii) correlate PNCs inside the cabin to those measured outside, and (iii) predict PNCs in the cabin based on those outside the cabin using a semi–empirical model. A fast response differential mobility spectrometer (DMS50) was employed in conjunction with an automatic switching system to measure PNCs and PNDs in the 5-560 nm range at multiple locations inside and outside the cabin at 10 Hz sampling rate over 10 seconds sequential intervals. Two separate sets of measurements were made at: (i) four seats in the car cabin during ~700 minutes of driving, and (ii) two points, one the driver seat and the other near the ventilation air intake outside the cabin, during ~500 minutes of driving. Results of the four–point measurements indicated that average PNCs at all for locations were nearly identical (i.e. 3.96, 3.85, 3.82 and 4.00×10^4 cm^{-3}). The modest difference (~0.1%) revealed a well-mixed distribution of nanoparticles in the car cabin. Similar magnitude and shapes of PNDs at all four sampling locations suggested that transformation processes (e.g. nucleation, coagulation, condensation) have minimal effect on particles in the cabin. Two–point measurements indicated that on average, PNCs inside the cabin were about 72% of those measured outside. Time scale analysis indicated that dilution was the fastest and dominant process in the cabin, governing the variations of PNCs in time. A semi-empirical model was proposed to predict PNCs inside the cabin as a function of those measured outside. Performance evaluation of the model against multiple statistical measures was within the recommended guidelines for atmospheric dispersion modelling. Trip average PNCs obtained using the model demonstrate a reasonably good correlation (i.e. $R^2 = 0.97$) with measured values.

Keywords: Car cabin exposure; Nanoparticles dispersion; Number and size distribution; Transformation processes; Ultrafine particles

---

[1]Corresponding author. Department of Civil and Environmental Engineering (C5), Faculty of Engineering and Physical Sciences (FEPS), University of Surrey, Guildford GU2 7XH, UK. Tel.: +44 1483 682762; fax: +44 1483 682135. E-mail addresses: P.Kumar@surrey.ac.uk, Prashant.Kumar@cantab.net

1. Introduction

Vehicle emissions are generally the major source of atmospheric nanoparticle pollution in urban areas and consequently make a very significant contribution to the associated adverse health effects (Bos et al., 2013; Donaldson et al., 2005; Hofmann, 2011; Oberdorster, 2000). The scale of such emissions can be estimated from the total number of road vehicles in operation worldwide, a figure put at more than 1 billion in 2010 (Sousanis, 2011). Road users are one of the most exposed groups and recent research by the authors (Joodatnia et al., 2013) demonstrated that freshly emitted nanoparticles comprised more than 99% of particle number concentrations (PNCs) inside a car cabin during journeys on typical UK urban roads. We continue that focus in this paper and investigate the relationship between nanoparticle pollution inside a car cabin and that prevailing outside, and the physical behaviour of particles within a cabin. We are referring nanoparticles to those below 300 nm here to represent the major population of PNCs.

A number of recent studies attempt to characterise passenger exposure to PNCs during commuting. In general, higher PNCs are reported in car cabins (4.9×10^4 cm^{-3}) compared with other transport modes such as buses (4.2×10^4 cm^{-3}) or cycles (3.4×10^4 cm^{-3}) (Int Panis et al., 2010; Knibbs et al., 2011; Knibbs and de Dear, 2010; Wang and Oliver Gao, 2011). Knibbs et al. (2011) highlight that the key determinants (e.g. ventilation system, routes, traffic parameters, meteorological conditions) should be taken into account prior to ranking different transport modes in respect to exposure level. Joodatnia et al. (2013) conducted car cabin measurements in a typical UK town (Guildford). They found that the close proximity to the tail pipe of the preceding vehicle, in slow moving and congested traffic conditions, was the dominant traffic parameter responsible for high PNC levels in the cabin. One second averaged PNC measurements were found to be up to two order of magnitude greater than hourly average values in the car cabin (Joodatnia et al., 2013).

A number of recent studies have also addressed the correlation between PNCs in a car cabin and those measured outside, as summarised in Table 1. The flux rate of nanoparticles into the car cabin is highly influenced by the air exchange rate (A_E) (Fruin et al., 2011; Hudda et al., 2012). Hudda et al. (2012) identified dominant factors which influence A_E and the ratio of PNCs in the car cabin to those measured outside the cabin; the latter is the so-called penetration factor (*I/O*). Regression analysis of 116 vehicles under different driving speeds and ventilation settings indicated that A_E is the dominant factor affecting *I/O* (Hudda et al., 2012). General consensus is that A_E increases when windows are kept open compared to closed windows conditions with the ventilation on. Fruin et al. (2011) measured A_E under recirculation fan setting for 63 vehicles and found that A_E increased at higher travelling speeds. However, this effect was more significant for older vehicles compared to newer ones (Fruin et al., 2011). This is possibly due to reduction of sealing efficiency of doors and windows in older cars, which causes them to be less air tight (Fruin et al., 2011; Knibbs et al., 2009). Zhu et al. (2007) measured PNCs in a cabin of a Volkswagen Jetta (model year 2000) on a Los Angeles freeway and reported *I/O* ~0.8 under the outside air intake fan setting (see Table 1). Zhu et al. (2007) show that the *I/O* decreases (i.e. ~0.4) in newer cars (e.g. Audi A4,

model year 2004) under the same ventilation conditions. Generally, higher penetration of nanoparticles into the cabin of old cars is experienced compared to newer cars (Tartakovsky et al., 2013; Zhu et al., 2007). Zhu et al. (2007) conclude that vehicle age plays a significant role in commuter protection to nanoparticles in the car cabin. Knibbs et al. (2010) measured PNCs outside and in the car cabin during trips in a tunnel in Sydney, and found the lowest *I/O* (0.84) for filter fitted vehicles, with the ventilation set to intake outside air into the car cabin. They also showed that the filtration efficiency was improved and *I/O* reduced further to 0.66 when lower fan settings were employed, see Table 1. Substantial reduction in *I/O* (i.e. to 0.08–0.47) was observed when the recirculation ventilation setting was employed (Knibbs et al., 2010). Knibbs et al. (2010) state that newer cars with built-in air filters generally offer greater passenger protection to external nanoparticles. A significant reduction in penetration factor is usually observed in driving modes with windows closed and fan set to recirculation. Despite attempts to identify influential factors on *I/O*, the general assumption is that *I/O* is constant for all size ranges and no quantitative method of estimating *I/O* for different particle sizes are yet reported in the literature.

Particles emitted from road vehicles undergo a series of complex transformation processes which are constantly competing against each other on different time scales (Ketzel and Berkowicz, 2004). Carpentieri and Kumar (2011) indicate that nucleation is the fastest ($\sim 10^{-7}$ -10^{-8} s) particle transformation process during the first stage of dispersion near the tail pipe. Except this initial dispersion stage, for almost all concentration levels near kerbsides in urban environments, the fastest process is dilution, $\sim 10^{-1}$–10^{-2} s (Ketzel and Berkowicz, 2004). Previous works have evaluated the time scales of particle transformation processes at different urban scales (i.e. street, vehicle wake), but similar studies do not currently exist for vehicle cabins. Therefore, measurements at high sampling frequencies (e.g. 1 second or faster) are essential to obtain a realistic insight of PNC levels, PNDs and transformation processes in car cabins. Such understanding will also provide an opportunity to study short–term personal exposure in car cabins.

In response to these research gaps, a fast response differential mobility spectrometer (Cambustion DMS50) was deployed in conjunction with an automated switching system to measure PNCs and PNDs at multiple points in and outside a car cabin. Measurements represent the driver and passenger seats, and in front of the bonnet outside the car cabin. This study analyses PNC distributions at four points in the car cabin. The study also assesses effects of transformation processes (i.e. coagulation, dry deposition) on PNCs and PNDs in the car cabin using fast response (500 milliseconds) measurements. Furthermore, a quantitative method of estimating *I/O* for different particle size and a semi–empirical model was proposed to link PNCs in the car cabin to those measured outside.

2. Methodology

2.1. Study design and route

Measurements were conducted on car journeys during May 2012 in Guildford town centre. Guildford is a typical UK town with about 137,200 inhabitants (OFNS, 2011).

Guildford Borough has reported a much higher car ownership (more than two cars per household) than the national level (~1.1) (Guildford-Borough, 2008). As in previous measurements in Guildford (Joodatnia et al., 2013), measurements were made on a 2.7 km long route that connects Guildford town centre to the University of Surrey (Fig. 1a). The maximum speed limit on the route was 48 km h^{-1}. The average speed of the test vehicle was 22±4 and 18±3 km h^{-1} during morning and afternoon journeys, respectively, with corresponding journey times of 7±2 and 10±3 minutes. The road characteristics and typical traffic condition are given in detail by Joodatnia et al. (2013).

2.2. Instrumentation and data collection

Measurements were made in the cabin of an unleaded petrol-fuelled car (Volkswagen Golf, 1998 registration; 1600cc). The total outdoor air flow rate (7.7×10^{-2} m^3 s^{-1}) were estimated by means of tracer gas technique as part of our earlier work (Joodatnia et al., 2013). All windows remained closed throughout the study periods, and the only source of ventilation was a fan-driven system (on medium speed; 2 of a scale of 1–4), which maintains an outdoor air flow rate of 4.2×10^{-2} m^3 s^{-1} into the cabin. The difference between the total air flow rate in the cabin and those provided by fan assisted ventilation is due to air leak through the cabin sealing. The experimental car was equipped with neither air conditioning nor a filter fitted ventilation system. It should be noted that a non–smoking driver was the only occupant in the car throughout the experiments.

Experiments were conducted using a DMS50, measuring number and size distributions of particles in the 5–560 nm range at a sampling frequency of 10 Hz with a 500 milliseconds response time. The DMS50 has recently been employed in studies within the same car cabin (Joodatnia et al., 2013) and for the on–board measurements (Carpentieri and Kumar, 2011). The instrument was found to perform well in these circumstances. Further details on the working principle, noise levels and application for ambient measurements can be found elsewhere (Kumar et al., 2010). An internal pump enclosed within the instrument maintained a sampling flow rate of 6.5 lit min^{-1} through electrically and thermally conductive sampling tubes. Short length (~0.50 m) sampling tubes, having 5 mm internal diameter, giving 0.3 s residence time, were employed to minimise particle losses (Kumar et al., 2008a). The instrument was calibrated by the manufacturer (Cambustion Ltd.) in January 2012, and, the measurements were conducted within the one year calibration validation period.

A DC power operated automated solenoid switching system was used in conjunction with the DMS50 for making the measurements at multiple locations (see Fig. 1b). The switching system was software controlled, allowing 10 s measurements at each location by redirecting the sampling flow among the locations. The first 2 s of data from each measurement was discarded in order to allow for sample clearance and the final 8 s of data was retrieved for analysis.

Two separate sets of measurements were made sequentially over 10 second intervals at: (i) four points in the car cabin, and (ii) at two points, one the driver's seat and the other near the ventilation air intake outside the car. The measurements in the cabin were conducted at near breathing height (i.e. 1.2 m above the car floor). A total of 78 runs were conducted for four

point measurements, in which 7 runs were discarded due to errors in data acquisition, providing about 700 minutes of measurements on the selected route. For two points measurements, a total of 50 runs was conducted, in which 1 run was discarded, giving about 500 minutes of measurements.

The ambient wind speed and direction, temperature and relative humidity were also monitored during the study period, together with the cabin temperature and humidity. The average meteorological conditions and cabin temperature and humidity are summarised in Table 2.

2.3. Semi-empirical model to predict PNCs in a car cabin

A semi-empirical model was developed to predict PNCs in the car cabin as a function of those measured just outside. Jamriska et al. (2000) introduced a mathematical model which calculates PNCs in an indoor environment (i.e. office building). Later, Knibbs et al. (2010) adopted this model for vehicles and we further modified this to take into account the car ventilation system (i.e. without both HVAC filtration and recirculation systems) and adopted for our work, as seen in Eq. (1). Detailed derivation of the model is provided in Supplementary Information (SI) Section S.1. The proposed model assumes that PNCs are "well-mixed" and losses due to transformation processes are modest. These assumptions were proved appropriate based on four-point measurements and time scale analysis (see Section 3). The losses within the ventilation system were treated by using the empirical constant *I/O*. He et al. (2007) suggest that to estimate declining PNCs, a semi-empirical constant (e.g. *I/O)* can be used to account for all the losses due to particle transformation processes, without distinguishing between them. Eq. (1) calculates PNCs in the cabin (N_{ci}) for particles in the size class i at any time (t_{n+1}) based on those measured or estimated outside (N_{Oi}) and inside the cabin in previous time step (t_n):

$$N_{ci}(t_{n+1}) = N_{oi}(t_n) \times (I/O)_i + (N_{ci}(t_n) - N_{oi}(t_n) \times (I/O)_i) \times e^{-A_E(\Delta t)} \quad (1)$$

Where A_E is the air exchange rate into the car cabin (see SI Section S.2.1). The subscript i indicate values (e.g. N_c, *I/O* and N_o) in the D_p to $D_p + d_p$ size range, with D_p and d_p being particle diameter and the increment between two sizes, respectively. Due to fluctuating nature of N_o, a time averaged value is employed at each time step.

2.3.1. Quantitative performance evaluation of the box model

A number of methods have been introduced in literature to evaluate the performance of models for different applications (e.g. research, forecasting) in fields such as air quality modelling (Chang and Hanna, 2004; Hanna et al., 1993; Thunis et al., 2011). Since each of proposed performance evaluation methods has its advantages and disadvantages, it is generally recommended to apply multiple techniques (Thunis et al., 2011). A number of performance indicators suggested by Hanna et al. (1993) for atmospheric dispersion models are adopted for our work. These includes Pearson correlation coefficient (R), the fraction of predictions within a factor of two of the measurements (FAC2), mean fractional bias (FB),

the normalized mean square error (NMSE), geometric mean bias (MG), the geometric variance (VG) (Chang and Hanna, 2004; Mazzoldi et al., 2008). The related formulas are given in the SI Section S.2.

A "perfect" model would give R, FAC2, MG and VG values equal to 1, and FB and NMSE values as 0 (Hanna et al., 1993). However, since dispersion and transport in the atmospheric environment are influenced by random characteristics of eddies in turbulent flows, it is impossible in general to model exactly what is measured. Therefore, due to the uncertainties in urban modelling applications, the acceptance criteria are relaxed, as described by Hanna et al. (1993):

- Pearson correlation coefficient between predicted and measured PNCs should be greater than 0.7 (i.e. $|R| \geq 0.7$).
- The fraction of predicted PNCs within a factor of two from those measured should be greater than 0.7 (i.e. $|FAC2| \geq 0.7$).
- The mean bias should be within ± 30% of the mean (i.e. 0.7 < MG < 1.3 and $|FB|$ <0.3).
- The random scatter of predicted PNCs should be within a factor of two of the mean (i.e. VG <1.6 and NMSE <4).

2.4. Time scale analysis of particle transformation processes in the car cabin

Time scale analysis is an approach to study the possible effects of particle transformation processes on PNCs and PNDs. The effect of different processes is highly dependent on the time scale (τ) of each, with the smallest time scale being the most effective (Ketzel and Berkowicz, 2004). The ratio of PNC (N; # cm^{-3}) and PNC variation in time ($\dot{N} = \frac{\partial N}{\partial t}$; # cm^{-3} s^{-1}) due to a transformation process (e.g. coagulation) is regarded as the time scale of that specific transformation process (e.g. τ_{coag}).

$$\tau = \left| \frac{N}{\dot{N}} \right| \quad (2)$$

The assumptions of the time scale analysis for dilution, coagulation, dry deposition and condensation processes are outlined below. The detailed analytical approach and calculation methodologies for these analyses are reported in the SI Section S.3 and related results and discussions in Section 3.3.

A_E was estimated using the tracer gas decay method as described by Bassett et al. (1981):

$$N_c(t_{n+1}) = N_c(t_n) e^{-A_E \Delta t} \quad (3)$$

A separate set of measurements were employed to estimate A_E. These measurements were conducted at a single point at the front passenger seat (Joodatnia et al., 2013).

Coagulation can occur due to Brownian motion, sedimentation, shear forces or Van der Waals interaction (Seinfeld and Pandis, 2006; Vignati et al., 1999). However, a Brownian motion induced coagulation process for polydisperse particles is considered in this study and

the estimates are made using the methodology described by Ketzel and Berkowicz (2004), see SI Section S.3.1.

Particle deposition in homogenous and isentropic turbulent flow onto cavity surfaces were calculated using the model introduced by Lai and Nazaroff (2000), as described in SI Section S.3.2. The model takes account of deposition of particles; (i) on all surfaces (i.e. horizontal and vertical) by Brownian and turbulent diffusion, and (ii) on horizontal surfaces by gravitational settling. It should be noted that PNCs are assumed to be uniformly distributed within the car cabin, except for the boundary layer adjacent to the surfaces (Lai and Nazaroff, 2000). The total cabin volume was estimated at 4 m^3, and the vertical, upward and downward facing horizontal surface areas were 6, 3.5 and 3 m^2, respectively.

Unlike other transformation processes (discussed in the previous paragraphs), which are mainly characterised by PNCs, condensation and nucleation processes both involve vapour concentration and phase conversion (i.e. gas to particle) processes (Ketzel and Berkowicz, 2004, 2005). Nucleation and condensation compete either to form new particles or to condense onto pre-existing particle surfaces, respectively (Jacobson and Seinfeld, 2004; Kulmala et al., 2004). Kittelson (1998) indicates that nucleation and condensation occur immediately in the vehicle exhaust plume during rapid cooling and mixing (dilution) of hot volatile vapours released from the tail pipe into the surrounding atmosphere. It is assumed that during the first seconds of release, tailpipe gas are below their saturation ratio due to rapid dilution and these initial nucleation/condensation processes are completed (Kittelson, 1998; Shi and Harrison, 1999). These processes are regarded as defining the emission (Ketzel and Berkowicz, 2004) and are not treated in this study. However, the condensational growth of particles in the car cabin is investigated here. The rate of PNC change (cm^{-3} s^{-1}) due to condensation is a function of the particle growth rate (GR) (Ketzel and Berkowicz, 2004; Kulmala et al., 2004). Ketzel and Berkowicz (2004) indicate that the possible existence of organic vapours accounts for the growth of emitted particles, and therefore, employed the range 1–10 nm h^{-1} to represent GR in urban areas. This range is applicable for particles smaller than 100 nm in diameter, those in the kinetic regime, while GR decreases in inverse proportional to the particle diameter for larger particles (Kerminen and Wexler, 1995; Ketzel and Berkowicz, 2004); see SI Section S.3.3 for details. Here, the maximum GR (i.e. J_0 = 10 nm h^{-1}) observed in urban areas is taken to approximate the time scale due to condensation process (τ_{cond}) in the car cabin.

3. Results and discussion

In order to ensure the quality of the data collected, sensitivity levels of the DMS50 were assessed by comparing the lowest level of PNDs that the instrument is capable to detect with the minimum PND measured along the route. PNDs for background (minimum) PNCs were found to be well above the lowest level of PNDs that the DMS50 is capable to detect for particle diameters above 7 nm. Further details of instrument signal–to–noise ratio are discussed in our recent study (Joodatnia et al., 2013).

3.1. PNC analysis

3.1.1. Four points measurements

Average PNCs at the four sampling locations are summarised in Table 3. The four–point measurements indicated that average PNCs are distributed approximately evenly at all four locations in the cabin; 3.96, 3.85, 3.82 and 4.00 $\times 10^4$ cm^{-3} at points P_1, P_2, P_3 and P_4, respectively. Despite great temporal variability of the data at each point, the average PNCs show insignificant differences (~0.1%) between four points. This indicates a relatively well mixed distribution of nanoparticles in the car cabin.

PNCs were divided into nucleation ($N_{5\text{-}30}$), accumulation ($N_{30\text{-}300}$) and coarse modes ($N_{300\text{-}560}$) for detailed inspection; the subscripts indicate particle diameter in nm. Average PNCs over all four locations indicates that particles in the 5–30 and 30–300 nm size ranges contribute to 35.3 and 64.5% of PNCs measured in the cabin, respectively. This left a negligible fraction (~0.2%) of particles in the 300–560 nm size ranges. PNC at both front and back seats indicated a similar proportion of nucleation and accumulation mode particles. Details of proportion of $N_{5\text{-}30}$, $N_{30\text{-}300}$ and $N_{300\text{-}560}$ at all four locations can be seen in SI Figs. S2–S3.

3.1.2. In and outside car cabin

Table 4 shows a summary of PNC measurements at two points: one in the car cabin (P_2) and the other outside (P_5). As shown in Section 3.1.1, PNCs in the car cabin environment are well mixed and average PNCs at P_2 are almost equal to those at other points in the cabin. Therefore, it can be assumed that PNC measurements at P_2 are representative of the whole cabin environment. Table 4 presents a summary of the penetration factor (*I/O*) for different particle size ranges. This suggests that average PNCs in the cabin ($2.72 \pm 1.03 \times 10^4$ cm^{-3}) are 72% of those measured outside. This result is consistent with the *I/O* value reported by other studies such as Knibbs et al. (2010), as summarised in Table 1, under the same ventilation condition and vehicle age.

The average *I/O* for the present work was computed as 0.55, 0.82 and 0.11 for particles in the 5–30, 30–300 and 300–560 nm size ranges, respectively. Fig. 2 indicates size–resolved penetration factors $(I/O)_i$ for particles in the 5-560 nm size range. Eq. (4) provides the best fitted line with coefficient of determination (R^2) about ~0.93 (see Fig. 2).

$$(I/O)_i = 0.15 \ln(D_p)_i + 0.175 \quad (4)$$

These results show that the penetration factor is far from constant for particles in 5–560 size range, with attenuation in the nucleation and accumulation modes and enhancement above 300 nm in diameter. The reductions for nucleation and accumulation mode particles are due to the greater diffusivity of these particles in comparison with particles over 300 nm (Seinfeld and Pandis, 2006), and also losses as a result of formation of larger particles due to coagulation of smaller particles in the ventilation system. The *I/O* values greater than unity for particles larger than 300 nm is probably indicative of re-suspension of these particles in the car cabin, and also the formation of larger particles by coagulation of smaller sizes. Eq. (4) can be used with Eq. (1) in order to predict PNCs in the cabin using measured values

outside the cabin. However, it should be noted that the analytical expression for size–resolved $(I/O)_i$ is strongly influenced by vehicle characteristics such as mileage, age, ventilation system/setting and vehicle air tightness. Therefore, this expression may only be used for similar vehicle and ventilation conditions. Careful consideration is required to apply Eq. (4) to other vehicles and different ventilation conditions.

Table 4 shows that, on average, the PNC weighted geometric mean diameters of all particles are ~48 and ~53 nm for those measured outside and in the cabin, respectively. This again highlights the fact that freshly emitted PNCs are possibly coagulated and grown in diameter to larger size by the time they reach the car cabin. This might be the reason of a greater proportion of PNCs in the accumulation mode (~74%) in the car cabin in comparison with those measured outside (~65%), see SI Section S.5.

As seen in Table 4, PNCs outside the cabin demonstrate greater fluctuations (standard deviation, St-Dev = $\pm$ 1.6×10^4 cm^{-3}) with time in comparison with those measured inside the cabin ($\pm$ 1.03×10^4 cm^{-3}). PNCs in the cabin show relatively lower rate of changes in comparison with those measured outside. This is due to the fact that dilution time scale in the cabin is about ~36 s (see Section 3.3). On the other hand, PNC changes outside the cabin are influenced by unsteady characteristics of ambient and traffic produced turbulence in street canyons which lead to relatively larger changes in PNCs outside (Kumar et al., 2008b). Similarly, Zhu et al. (2007) reported greater variations of PNCs outside the cabin (St-Dev = $\pm$ 2.4×10^4 cm^{-3}) compared to those measured inside ($\pm$ 0.93×10^4 cm^{-3}). Results reported by Zhu et al. (2007) indicate greater St-Dev for PNCs measured outside the cabin compared to those measured in Guildford. This is presumably due to fact that both traffic induced turbulence and wind speed are greater in highways compare with those in street canyons in city environments, where the ventilation is reduced relatively (Buonanno et al., 2011).

3.1.3. Variations of PNCs in the cabin

Table 5 summarises average PNC measurements at P_2 in the car cabin during a total of 150 trips on the same route. These measurements were conducted during three campaigns in winter 2011 and in spring 2012. Measurements during winter 2011 were reported previously by Joodatnia et al. (2013). These measurements were conducted in January and February 2011, but as the temperature variations during the time of the experiments were relatively small in comparison with those in spring, they were treated as one set of measurements, denoted as WC hereafter. Spring period measurements were conducted during third (17-18th) and fourth (22-23rd) weeks of May 2012 and are denoted as SC1 and SC2, respectively. Average PNCs (5.87 ± 4.06 $\times10^4$ cm^{-3}) measured during the WC differ significantly from those measured during SC1 and SC2; i.e. 3.85 ± 3.07 $\times10^4$ and 2.72 ± 1.03 $\times10^4$ cm^{-3}, respectively. Moreover, PNCs in the 5–30 nm size range during WC are 2.4 and 4.7 times greater than those measured during SC1 and SC2, respectively. On the other hand, ratios for PNCs in the 30–300 nm size range are almost unity (see Table 5). As discussed in Section 1, there are many factors affecting the variations of PNCs in the car cabin. Important factors when comparing the spring and winter seasons are likely to be the traffic intensity and meteorological conditions (e.g. temperature and humidity).

Lower ambient temperatures were reported during the WC (1–4 ^{o}C) than during SC1 (10–14 ^{o}C) and SC2 (15–25 ^{o}C; Table 2). This lower temperature could be a possible factor responsible for the larger peaks in the nucleation mode during the WC (see Table 5). However, the coefficient of determination indicates only a weak correlation between ambient temperature and variations in PNCs in the car cabin ($R^2 \sim 0.34$) (see SI Section S.4). Relative humidity also influences PNCs. However, the variations of relative humidity during the measurements were limited and no connection with the PNCs was distinguished (see Table 5). Similarly, wind speed during the time of measurements did not vary significantly.

A significant reduction in traffic intensity was observed during SC1 and SC2. Consequently, the test car was driven in less congested conditions with only occasional stop and go at traffic lights and junctions. Our earlier work (Joodatnia et al., 2013) indicated that large variations in PNC measurements in the car cabin were observed due to travel speed, traffic intensity and proximity of the experimental car to other vehicles. Moreover, the speed of travel strongly relates to congestion. In less congested zones, at free flowing traffic, greater traffic induced turbulence is experienced due to the higher average speed of vehicles. Therefore, a greater dilution rate of particles occurs at street level, which possibly contributes to the observed reduction in PNC levels in the car cabin.

Overall, it should be noted that the experiments were conducted on a limited number of days during the winter and spring periods, 2 and 4 days, respectively. Therefore, no definitive conclusions can be drawn for these observations alone, but it is relevant to assess the results in the light of the wider published literature. However, key factors determining temporal PNC peaks and high average PNCs in the car cabin have shown to be local traffic intensity and driving conditions (Joodatnia et al., 2013; Knibbs et al., 2011). Knibbs et al. (2011) reviewed PNC measurements in a number of transport microenvironments (i.e. bus, taxi and train) and concluded that the connection between PNCs and meteorological factors (i.e. ambient temperature, humidity, wind speed) was not well defined and found to be mainly location (e.g. city) dependant. Thus, it can be concluded the most likely factor for the reduction in PNCs in the car cabin during the SC1 and SC2 is the significant reduction in traffic intensity and consequently driving on less congested roads in comparison with WC.

3.2. PND analysis

3.2.1. Four points measurements

Fig. 3a shows averaged PNDs at the four sampling positions in the car cabin during 71 journeys. The four points are denoted as P_1, P_2, P_3 and P_4. The bimodal PNDs have peaks centred at about the 10 nm ($2.06\pm2.05 \times 10^4$ cm^{-3}) and 60 nm ($4.63\pm3.99 \times 10^4$ cm^{-3}) in the nucleation and accumulation modes, respectively (see Fig. 3a). Figs. 3b-e show that despite great variations in PNDs at each point, the average distributions are similar in shape and magnitude. This suggests that the variation of PNCs in the car cabin is mainly due to dilution effects. These results broadly agree with the literature for other spatial scales (e.g. vehicle wake, street canyons), where dilution is reported as the dominant process (Kumar et al., 2009, 2011). Time scale analyses of particle transformation processes are carried out in Section 3.3 to investigate this finding furthermore.

3.2.2. In and outside car cabin

Fig. 4 shows averaged PNDs outside and inside the cabin during 49 journeys over the selected route. The two sets of PND measurements are similar for particles in the 30–300 nm size range, with *peak* values 4.43±2.13 and 3.64±1.67 $\times 10^4$ cm^{-3} at about 75 nm, for outside and car cabin measurements, respectively. However, for particles smaller than 30 nm, these values were 2.07±1.73 $\times 10^4$ cm^{-3} at 10 nm and 11.1±5.75 $\times$ 10^4 cm^{-3} at about the 7 nm, for outside and in cabin measurements, respectively. As previously discussed in Section 3.1.2 and shown by Fig. 4, the ratio of external to internal PNDs is greater in the nucleation mode particles than those in the accumulation mode. These highlight that PNDs for both inside and outside the cabin demonstrate almost identical bimodal shape, despite the differences in their magnitudes.

3.3. Time scale analysis

Using the methods introduced in Section 2.4, time scales of the particle transformation processes were calculated for particles in the 5–560 nm size range in the car cabin. Table 6 lists the shortest time scale associated with each processes.

For the specified ventilation setup (see Section 2.2), the outdoor air exchange rate into this car cabin was found ≈100±38 h^{-1}. The variation in A_E in the car cabin under a fixed ventilation setting is mainly due to driving speed (Fruin et al., 2011; Hudda et al., 2012). It can be seen that the average dilution time scale in the car cabin is about 36 s. It should be noted that this estimation is only valid under the current ventilation settings, and would differ if the ventilation conditions (i.e. fan setting, windows condition) were altered. It should be noted that as discussed previously in Section 2.4, the time scale of condensation processes is a function of growth rate. Therefore, the value of τ_{cond} based on GR 10 nm h^{-1} is a factor of 10^{17} s by definition, which is much longer than dilution time scale (~36 s). However, τ_{cond} is included in the time scale analysis for the sake of completeness.

Time scale analyses for particles in 5–560 nm size range are shown in Fig. 5. It can be seen that dilution process is the shortest process (~36 s) in the car cabin. Generally, for other transformation processes (i.e. coagulation, dry deposition and condensation), the fastest processes occur at the smallest size particle, with coagulation for particles below 10 nm being the fastest (10^3 s) of all. Fig. 5 indicates that particle losses due to coagulation are faster than dry deposition for particles below 100 nm in size. However, the trend is reversed for particles larger than 100 nm. The time scale analysis indicates that coagulation (~620 s), dry deposition (~830 s) and condensation (~3.5×10^{17} s) processes are much slower than dilution (~36 s). Therefore, it can be concluded that dilution is the dominant process in the car cabin. This is in agreement with our previous finding based on PNCs and PNDs at all four sampling locations.

Direct comparison of these results with other studies was not possible due to the lack of similar time scales analysis available in published literature. However, the other recent studies have reported similar findings (Fruin et al., 2011; Hudda et al., 2012; Hudda et al., 2011; Knibbs et al., 2009). For instance, in a different urban setting, Vignati et al. (1999)

concluded that coagulation processes do not have a significant effect on the size distribution in exhaust plumes due to the rapid dilution that takes place. Our findings for the car cabin also seem to agree with studies near street kerbsides which report dilution as the dominant process, with other transformation processes showing negligible effect on PNC levels (Ketzel and Berkowicz, 2004; Kumar et al., 2008c).

3.4. Measured versus modelled PNCs in cabin

Having found the car cabin to be a well–mixed environment (Section 3.1.1) and with dilution as the dominant process influencing PNCs (Section 3.3), the semi–empirical mathematical model introduced in Section 2.3 (Eq. 1) is used to predict PNCs from those measured outside. In order to evaluate the performance of the proposed model against measurements, the total 49 trips were split into two segments by a random selection method. A total of 25 trips was employed in order to obtain size-resolved penetration factors $(I/O)_i$, and 24 remaining were used for comparison of measured and predicted PNCs. Using Eq. (1), in-cabin PNCs (N_{ci} (t_{n+1})) for particles in 5–560 nm size range (i) were estimated in 10 s (t) increments during 24 trips. For each time step, the initial internal PNCs (N_{ci} (t_n)) and 10 seconds averaged external PNCs (N_{Oi}) are obtained from actual measured values in the previous time step. Fig. 6 shows that the predictions provide good agreement with measured PNCs in the 5–560 nm size range, with coefficient of determination close to unity (R^2 = 0.97). However, there are over and under predictions (± 10%) in some cases that are shown above and under the 1:1 ratio line in Fig. 6. These results are similar to those reported previously by Knibbs et al. (2010) in which they used a similar model under different ventilation settings.

To study the performance of the proposed model further, predicted averaged PNCs in the car cabin were compared with those measured for 10000 seconds at 10 seconds time steps. The comparisons were conducted for $N_{5\text{-}30}$, $N_{30\text{-}300}$, $N_{300\text{-}560}$ and $N_{5\text{-}560}$. Fig. 7 indicates that the R^2 between predicted and measured PNCs for the all the size ranges are ~0.6, which is considerably smaller than that for trip average PNCs (R^2 = 0.97). This highlights the fact that although the model performs well for average values for each journey, its performance is significantly reduced on individual time steps. Under and over predictions by the model are mainly due to the fact that a constant A_E was employed for each time step. However, A_E changes due to variations in travel speed in real operational conditions as discussed in Section 1. Therefore, it can be concluded that despite good performance for averaged PNCs, the model might be further improved by using appropriate A_E values at each time step. Existing quantitative models, such as those proposed by Hudda et al. (2012) can be implemented in Eq. (1) to estimate A_E under different ventilation systems and driving modes. Such estimation of A_E according to driving modes would assist to predict PNCs in the cabin more accurately. This would be highly beneficial where ventilation settings vary over the time and a more accurate approximation of personal exposure is required.

Using the statistical measures introduced in Section 2.3, the operational performance of the model was assessed for the whole data set (10000 seconds) at 10 seconds time steps. Table 7 indicates that the fraction of predicted PNCs within a factor of two (FAC2) of the measured

values is greater than 0.9 for all size ranges (i.e. 5–30, 30–300, 300–560 and 5–560 nm). The mean FB for all size ranges are well within ± 30% of the mean and the MG values are very close to the value of one. The VG for all size ranges indicate that the predicted PNCs are scattered within a FAC2 of those measured. The NMSE values state that the random scatters of predicted PNCs are about a factor of two of those measured. It can be concluded that despite the scattered over and under predicted results, generally, the given results by the model show good correlation with measured values.

Fig. 8a shows predicted and measured averaged PNCs in the car cabin for 10000 seconds at 10 seconds time steps. The complete comparison of data for different size ranges are shown in SI Figs. S4–S7. In order to examine the performance of the model more closely, the comparison for three trips is shown in Figs. 8b–d. These three cases demonstrate the best prediction (Fig. 8b), maximum under prediction (Fig. 8c) and maximum over predictions (Fig. 8d). Figs. 8c and d show the test cases in which the averaged PNCs in the 5–560 nm size range were the most under and over predicted values by 13 and 11%, respectively. Fig. 8b demonstrates that the modelled PNCs in most time steps were very close to the measured values. However, there are a few under or over predicted values, which are far from measured values (see Fig. 8b). As discussed previously, these under and over predicted values occur because of change in the actual A_E in the cabin due to travel at different speeds, respectively.

4. Conclusions and future work

Measurements of particles in the 5–560 nm size range were conducted using a fast response differential mobility spectrometer (DMS50) in conjunction with an automated solenoid switching system. Measurement were conducted at 10 Hz sampling rate over sequential 10s intervals (i) at four points in the car cabin, and (ii) at two points, one the driver seat, and the other near the ventilation air intake outside the cabin. The four point and two point measurements were conducted during ~700 and ~500 minutes of driving, respectively. The data set was used to investigate average PNC and PND variations in space and time at multiple locations inside and outside the car cabin.

Four-point measurements in the car cabin showed that PNCs at the front seats and the rear seats were almost identical. This indicates that the car cabin is a well-mixed microenvironment. Average PNDs at the four points were almost identical, which suggests that nanoparticles in the car cabin do not change size due to transformation processes (e.g. nucleation, coagulation, condensation). It should be noted that the estimated total cabin volume of the Volkswagen Golf was about 4 m^3, which is relatively small in comparison with other transport microenvironments (e.g. busses, trains). Therefore, the conclusions might not extend to these environments and measurements at multiple locations would need to be conducted to decide the matter.

Two–point measurements revealed that the ratio of internal to external average PNCs was about 0.72 (*I/O*). This is in agreement to those reported for similar vehicles age and mileage under the same ventilation setting. An expression was proposed to estimate size-resolved *I/O* as a function of particle size diameter. This expression is not universal and will depend

strongly on the vehicle characteristics (i.e. vehicle air tightness, age, mileage and ventilation setting/system). Therefore, the given expression should be used with care for other vehicles and ventilation settings/systems. It will be useful to examine the relation with different ventilation systems and vehicles types.

Time scale analysis showed that dilution was by far the shortest process in the car cabin and that the variation of PNCs was almost entirely due to this process. This finding is in agreement with previous studies which identified dilution as the dominant process. It should be noted that the conclusions of the time scale analysis is strongly influenced by ventilation setting and systems. Therefore, such analysis should be undertaken to extend this conclusion to other transport microenvironments with different ventilation setting/systems.

A semi-empirical model was developed using the size-resolved *I/O*. The model predicted PNCs in the car cabin based on those measured outside. The trip average PNCs predicted by the semi-empirical model showed good correlation (i.e. $R^2 = 0.97$) with measured values. The operational performance of the model for particles in different size ranges (i.e. 5–30, 30–300, 300–560 nm) was assessed over 10,000 seconds at 10 seconds time steps using standard statistical measures. The model performance for all particle size ranges was within the accepted criteria for urban air quality modelling. A constant air exchange rate (A_E) was employed as an input to the model despite the fact that A_E actually changes as a function of driving speed. The operational performance of the model can probably be improved by using a time dependant air exchange rate instead of the mean value. Overall, for future work, the modified semi-empirical box model should be examined against different ventilation systems and vehicles types.

5. Acknowledgements

This work is supported by the EPSRC DTA Grant. Thanks also to Surrey University for instrument grant and to Dr. Paul Hayden and Mr. Alistair Reynolds for their help during the experimental campaigns.

6. References

Bassett, M.R., Shaw, C.Y., Evans, R.G., 1981. Appraisal of the sulphur hexafluoride decay technique for measuring air infiltration rates in buildings. ASHRAE Transanctions 87, 361-373.

Bos, I., De Boever, P., Vanparijs, J., Pattyn, N., Panis, L.I., Meeusen, R., 2013. Subclinical effects of aerobic training in urban environment. Medical and Science in Sport and Exercise, In Press, DOI: 10.1249/MSS.0b013e31827767fc

Buonanno, G., Fuoco, F.C., Stabile, L., 2011. Influential parameters on particle exposure of pedestrians in urban microenvironments. Atmospheric Environment 45, 1434-1443.

Carpentieri, M., Kumar, P., 2011. Ground-fixed and on-board measurements of nanoparticles in the wake of a moving vehicle. Atmospheric Environment 45, 5837-5852.

Chang, J.C., Hanna, S.R., 2004. Air quality model performance evaluation. Meteorology and Atmospheric Physics 87, 167-196.

552 Donaldson, K., Tran, L., Albert Jimenez, L.A., Duffin, R., Newby, D.E., Mills, N., MacNee,
553 W., Stone, V., 2005. Combustion-derived nanoparticles: A review of their toxicology
554 following inhalation exposure. Particle & Fibre Toxicology 5/6, 553-560.
555 Fruin, S.A., Hudda, N., Sioutas, C., Delfino, R.J., 2011. Predictive Model for Vehicle Air
556 Exchange Rates Based on a Large, Representative Sample. Environmental Science &
557 Technology 45, 3569-3575.
558 Guildford-Borough, 2008. State of Guildford Borough report. Guildford-Borough, Guildford.
559 Hanna, S.R., Chang, J.C., Strimaitis, D.G., 1993. Hazardous gas model evaluation with field
560 observations. Atmospheric Environment. Part A. General Topics 27, 2265-2285.
561 He, C., Morawska, L., Taplin, L., 2007. Particle Emission Characteristics of Office Printers.
562 Environmental Science & Technology 41, 6039-6045.
563 Hofmann, W., 2011. Modelling inhaled particle deposition in the human lung—A review.
564 Journal of Aerosol Science 42, 693-724.
565 Hudda, N., Eckel, S.P., Knibbs, L.D., Sioutas, C., Delfino, R.J., Fruin, S.A., 2012. Linking
566 in-vehicle ultrafine particle exposures to on-road concentrations. Atmospheric
567 Environment 59, 578-586.
568 Hudda, N., Kostenidou, E., Sioutas, C., Delfino, R.J., Fruin, S.A., 2011. Vehicle and Driving
569 Characteristics That Influence In-Cabin Particle Number Concentrations.
570 Environmental Science & Technology 45, 8691-8697.
571 Int Panis, L., de Geus, B., Vandenbulcke, G., Willems, H., Degraeuwe, B., Bleux, N., Mishra,
572 V., Thomas, I., Meeusen, R., 2010. Exposure to particulate matter in traffic: A
573 comparison of cyclists and car passengers. Atmospheric Environment 44, 2263-2270.
574 Jacobson, M.Z., Seinfeld, J.H., 2004. Evolution of nanoparticle size and mixing state near the
575 point of emission. Atmospheric Environment 38, 1839-1850.
576 Jamriska, M., Morawska, L., Clark, B.A., 2000. Effect of Ventilation and Filtration on
577 Submicrometer Particles in an Indoor Environment. Indoor Air 10, 19-26.
578 Joodatnia, P., Kumar, P., Robins, A., 2013. The behaviour of traffic produced nanoparticles
579 in a car cabin and resulting exposure rates. Atmospheric Environment 65, 40-51.
580 K. Lai, A.C., Nazaroff, W.W., 2000. Modeling indoor particle deposition from Turbulent
581 flow onto smooth surfaces. Journal of Aerosol Science 31, 463-476.
582 Kerminen, V.M., Wexler, A.S., 1995. Growth laws for atmospheric aerosol particles: an
583 examination of the bimodality of the accumulation mode. Atmospheric Environment
584 29, 3263-3275.
585 Ketzel, M., Berkowicz, R., 2004. Modelling the fate of ultrafine particles from exhaust pipe
586 to rural background: an analysis of time scales for dilution, coagulation and deposition.
587 Atmospheric Environment 38, 2639-2652.
588 Ketzel, M., Berkowicz, R., 2005. Multi-plume aerosol dynamics and transport model for
589 urban scale particle pollution. Atmospheric Environment 39, 3407-3420.
590 Kittelson, D.B., 1998. Engines and nanoparticles: a review. Journal of Aerosol Science 29,
591 575-588.
592 Knibbs, L.D., De Dear, R.J., Atkinson, S.E., 2009. Field study of air change and flow rate in
593 six automobiles. Indoor Air 19, 303-313.
594 Knibbs, L.D., Cole-Hunter, T., Morawska, L., 2011. A review of commuter exposure to
595 ultrafine particles and its health effects. Atmospheric Environment 45, 2611-2622.

596 Knibbs, L.D., de Dear, R.J., 2010. Exposure to ultrafine particles and PM2.5 in four Sydney
597 transport modes. Atmospheric Environment 44, 3224-3227.
598 Knibbs, L.D., de Dear, R.J., Morawska, L., 2010. Effect of Cabin Ventilation Rate on
599 Ultrafine Particle Exposure Inside Automobiles. Environmental Science & Technology
600 44, 3546-3551.
601 Kulmala, M., Vehkamäki, H., Petäjä, T., Dal Maso, M., Lauri, A., Kerminen, V.M., Birmili,
602 W., McMurry, P.H., 2004. Formation and growth rates of ultrafine atmospheric
603 particles: a review of observations. Journal of Aerosol Science 35, 143-176.
604 Kumar, P., Fennell, P., Symonds, J., Britter, R., 2008a. Treatment of losses of ultrafine
605 aerosol particles in long sampling tubes during ambient measurements. Atmospheric
606 Environment 42, 8819-8826.
607 Kumar, P., Fennell, P., Britter, R., 2008b. Effect of wind direction and speed on the
608 dispersion of nucleation and accumulation mode particles in an urban street canyon.
609 Science of the Total Environment 402, 82-94.
610 Kumar, P., Fennell, P., Langley, D., Britter, R., 2008c. Pseudo-simultaneous measurements
611 for the vertical variation of coarse, fine and ultra fine particles in an urban street
612 canyon. Atmospheric Environment 42, 4304-4319.
613 Kumar, P., Robins, A., Britter, R., 2009. Fast response measurements of the dispersion of
614 nanoparticles in a vehicle wake and a street canyon. Atmospheric Environment 43,
615 6110-6118.
616 Kumar, P., Robins, A., Vardoulakis, S., Britter, R., 2010. A review of the characteristics of
617 nanoparticles in the urban atmosphere and the prospects for developing regulatory
618 controls. Atmospheric Environment 44, 5035-5052.
619 Kumar, P., Ketzel, M., Vardoulakis, S., Pirjola, L., Britter, R., 2011. Dynamics and
620 dispersion modelling of nanoparticles from road traffic in the urban atmospheric
621 environment—A review. Journal of Aerosol Science 42, 580-603.
622 Mazzoldi, A., Hill, T., Colls, J.J., 2008. CFD and Gaussian atmospheric dispersion models: A
623 comparison for leak from carbon dioxide transportation and storage facilities.
624 Atmospheric Environment 42, 8046-8054.
625 OFNS, 2011. Office of National Statistics. Census, Population and Household Estimates for
626 England and Wales. Office for National Statistics, UK.
627 Oberdorster, G., 2000. Toxicology of ultrafine particles: in vivo studies. Philosophical
628 Transactions of the Royal Society of London A 358, 2719-2740.
629 Seinfeld, J.H., Pandis, S.N., 2006. Atmospheric Chemistry and Physics - From Air Pollution
630 to Climate Change (2nd Edition). John Wiley & Sons.
631 Shi, J.P., Harrison, R.M., 1999. Investigation of ultrafine particle formation during diesel
632 exhaust dilution. Environmental Science and Technology 33, 3730-3736.
633 Sousanis, J., 2011. World Vehicle Population Tops 1 Billion Units, 15.08..2011 ed. Ward's
634 Automotive Group.
635 Tartakovsky, L., Baibikov, V., Czerwinski, J., Gutman, M., Kasper, M., Popescu, D.,
636 Veinblat, M., Zvirin, Y., 2013. In-vehicle particle air pollution and its mitigation.
637 Atmospheric Environment 64, 320-328.
638 Thunis, P., Georgieva, E., Galmarini, S., 2011. A procedure for air quality models
639 benchmarking, Models benchmarking. Joint Research Centre, Ispra, Forum for Air
640 Quality Modelling in Europe.

641 Vignati, E., Berkowicz, R., Palmgren, F., Lyck, E., Hummelshøj, P., 1999. Transformation of
642 size distributions of emitted particles in streets. Science of the Total Environment 235,
643 37-49.
644 Wang, X., Oliver Gao, H., 2011. Exposure to fine particle mass and number concentrations in
645 urban transportation environments of New York City. Transportation Research Part D:
646 Transport and Environment 16, 1361-9209.
647 Zhu, Y., Eiguren-Fernandez, A., Hinds, W.C., Miguel, A.H., 2007. In-cabin commuter
648 exposure to ultrafine particles on Los Angeles freeways. Environmental Science and
649 Technology 41, 2138-2145.
650
651
652
653

Citation details:
Joodatnia, P., Kumar, P., Robins, A., 2013. Fast response sequential measurements and modelling of nanoparticles inside and outside a car cabin. Atmospheric Environment 71, 364-375. http://dx.doi.org/10.1016/j.atmosenv.2013.02.028

Figure captions

Fig. 1: (a) Map of the study route, and (b) schematic diagram of experimental set-up in the car. The DMS50 and solenoid switching system were placed on the back seat. Number '1' indicates the sampling point at the driver position and numbers '2-4' at the passenger seats. Number '5' indicates the measurement point outside the car cabin. Configurations 1-4 were used for 'four-point' measurements, and points 2 and 5 were employed for in and outside cabin experiment. Tube positions are purely illustrative, for the sake of clarity.

Fig. 2: Average ratio of size-resolved PNCs in the cabin to those measured outside the cabin during 49 trips. Size-resolved PNCs (N_i) indicate concentration in the D_p and $D_p + d_p$ size range.

Fig. 3: (a) Averaged PNDs at the four locations, P_1, P_2, P_3 and P_4 in the cabin during the 71 journeys; (b) – (e) Averaged PNDs with relevant standard deviation bars at locations P_1-P_4, respectively. Only the positive standard deviation bars are included for the sake of clarity.

Fig. 4: Averaged PNDs outside and inside the cabin during 49 journeys; marked by "Out" and "Cabin", respectively.

Fig. 5: Average time scales for dilution, coagulation, dry deposition and condensation processes for particles in the 5–560 nm size range in the car cabin.

Fig. 6: Predicted and measured average PNCs in the cabin for 24 trips.

Fig. 7: Predicted and measured average size-resolved PNCs in the cabin for 10000 seconds at 10 seconds time steps; for particles in (a) 5–560 (b) 5–30, (c) 30–300 and (d) 300–560 nm size ranges. Dashed lines indicates the predicted PNCs within a factor of two (FAC2) of those measured. Dash dot line shows the data trend line.

Fig. 8: Predicted and measured averaged PNCs in 5–560 nm size range in the cabin at 10 seconds time steps for (a) 10000 seconds, and three journeys; in which PNCs, obtained by the model were on average (b) ~99%, (c) ~87% and (d) ~111% of those measured.

680

681 # List of Tables

Table 1: Summary of results of cabin to outside particle concentration ratio (*I/O*).

Study	Automobile	Model year	Odometer (×1000 km)	HVAC filter	AC	Ventilation condition[a]	*I/O*
Zhu et al. (2007)	Volkswagen Jetta	2000	-	Yes	Yes	A B C	0.8 0.7 0.6
Zhu et al. (2007)	Audi -	2004	-	Yes	Yes	A B C	0.35 0.5 0.18
Zhu et al. (2007)	PT Cruiser	2005	-	Yes	Yes	A B C	0.18 0.3 0.05
Knibbs et al. (2010)	Mazda 121	1989	160	No	No	A B C D	0.95 1.04 0.47 0.39
Knibbs et al. (2010)	Mitsubishi Magna	1998	138	No	No	A B C	0.89 1.01 0.29
Knibbs et al. (2010)	Toyota Hilux	2005	11	No	Yes	A B C	0.91 1.04 0.25
Knibbs et al. (2010)	Volkswagen Golf	2005	17	Yes	Yes	A B C D	0.66 0.84 0.08 0.17
Knibbs et al. (2010)	Subaru Outback	2007	11	Yes	Yes	A B C D	0.88 0.91 0.45 0.68
Hudda et al. (2011)	Ford Contour	1999	116	No New Used	Yes	A D A D A D	0.6 0.11 0.64 0.07 0.53 0.06
Hudda et al. (2011)	Honda Civic	2009	22	No New Used	Yes	A D A D A D	0.67 0.08 0.66 0.04 0.67 0.03
Hudda et al. (2011)	Toyota Prius	2010	3.2	No New Used	Yes	A D A D A D	0.6 0.05 0.57 0.03 0.52 0.02
Hudda et	Toyota	2010	11	No	Yes	A	0.51

al. (2011)	Prius			New		A	0.47
				Used		A	0.41
This study	Volkswagen Golf	1998	150	No	No	B	0.72[b]

A. Outside air intake (low fan/off), no recirculation
B. Outside air intake (medium fan), no recirculation
C. Outside air intake (low fan), with recirculation on
D. Indoor air recirculation only, no outdoor air intake.

[a] All windows closed.
[b] Size resolved penetration factor for particles with diameter in 5-560 nm size range are given in Section 3.1.2.

682
683

Table 2: Meteorological and environmental conditions during experiments. AM and PM correspond to measurements during morning and afternoon, respectively.

		Ambient				Car cabin	
Date		Wind speed ($m\ s^{-1}$)	Wind direction	Temperature (C^o)	Humidity (%)	Temperature (C^o)	Humidity (%)
28.01.2011	AM	5.5	NE	1	57	-	-
	PM	5.5	NE	1	57	-	-
18.02.2011	AM	3.5	SE	6	84	-	-
	PM	5.0	SE	6	79	-	-
17.05.2012	AM	4.5	SE	10	60	20	40
	PM	4.0	SE	14	55	25	30
18.05.2012	AM	4.0	SE	11	85	28	30
	PM	3.0	SE	14	80	25	40
22.05.2012	AM	4.5	NW	15	70	25	55
	PM	5.0	N	25	60	28	35
23.05.2012	AM	3.5	N	18	40	24	30
	PM	2.5	N	25	25	34	20

684
685

686
687

Table 3: Summary of results from the 4 sampling points. The results are averaged values for 71 journeys.

ID	PNC ($\times 10^4$ cm^{-3})				GMD (nm)			
	$N_{5\text{-}560}$	St-Dev	$N_{5\text{-}30}$	$N_{30\text{-}300}$	$N_{5\text{-}560}$	St-Dev	$N_{5\text{-}30}$	$N_{30\text{-}300}$
P_1	3.96	3.13	1.38	2.57	42.89	9.42	13.69	77.15
P_2	3.85	3.07	1.36	2.49	42.69	9.17	13.60	77.33
P_3	3.82	3.28	1.31	2.51	43.23	8.91	13.75	77.21
P_4	4.00	4.23	1.38	2.61	42.75	8.96	13.73	77.08
C	3.96	3.37	1.40	2.55	42.47	9.33	13.71	77.18

Note: P_1, P_2...refer to measurements at points 1, 2...in the car cabin, respectively, and C refers to the average of measurements at all 4 points (Cabin). $N_{5\text{-}560}$, $N_{5\text{-}30}$ and $N_{30\text{-}300}$ refer to PNCs in the 5–560, 5–30 and 30–300 nm size ranges, respectively. St-Dev and GMD refer to standard deviation of PNCs/GMDs and PNC weighted geometric mean diameter in the 5–560 nm size range, respectively.

688
689

Table 4: Summary of results from the 2 points measurements. Here, "cabin" and "outside" refer to measurements in the car cabin (P_2) and outside the cabin (P_5), respectively. *I/O* refers to cabin to outside particle concentration ratio.

ID	PNC ($\times 10^4$ cm^{-3})				GMD (nm)			
	$N_{5\text{-}560}$	St-Dev	$N_{5\text{-}30}$	$N_{30\text{-}300}$	$N_{5\text{-}560}$	St-Dev	$N_{5\text{-}30}$	$N_{30\text{-}300}$
Outside	3.75	1.62	1.29	2.45	48.34	9.54	12.81	85.56
Cabin	2.72	1.03	0.7	2.00	53.44	11.14	12.87	86.35
I/O	0.72	-	0.55	0.82	1.11	-	1.0	1.01

690
691

692

Table 5: Measurements at P_2 during the 4 points measurements in spring and those measured at the same location previously during winter period.

ID	PNC ($\times 10^4$ cm^{-3})				GMD (nm)			
	$N_{5\text{-}560}$	St-Dev	$N_{5\text{-}30}$	$N_{30\text{-}300}$	$N_{5\text{-}560}$	St-Dev	$N_{5\text{-}30}$	$N_{30\text{-}300}$
Winter[a]	5.87	4.06	3.28	2.52	33.27	2.58	13.23	71.45
Spring[b]	3.85	3.07	1.36	2.49	42.7	9.17	13.6	77.3
Spring[c]	2.72	1.03	0.7	2.00	53.44	11.14	12.87	86.35

[a]Joodatnia et al., (2013): January, February 2011

[b]Four points measurements 17-18th of May 2012

[c]In and outside cabin measurements 22-23rd of May 2012

693

694

Table 6: Time scale analyses for dilution, coagulation, dry deposition and condensation processes in the car cabin. SI stands for supplementary information.

	Dilution	Coagulation	Dry deposition	Condensation
Equation no.	2	SI (Eq. 18)	SI (Eq. 26)	SI (Eq. 29)
Shortest τ (s)	36	620	830	3.5×10^{17}

695

Table 7: Statistical measures to indicate the operational performance of the box model.

Size range	R	FAC2	FB	NMSE	MG	VG
$N_{5\text{-}30}$	0.84	0.95	0.026	0.36	0.97	1.13
$N_{30\text{-}300}$	0.81	0.98	0.003	0.24	1.00	1.06
$N_{300\text{-}560}$	0.75	0.92	-0.032	0.20	0.95	1.18
$N_{5\text{-}560}$	0.81	0.98	-0.005	0.20	1.00	1.06

Note: Pearson correlation coefficient (R), the fraction of predictions within a factor of two of the measurements (FAC2), mean fractional bias (FB), normalized mean square error (NMSE), geometric mean bias (MG), the geometric variance (VG).

696

Figure 1 (Colour).pptx

a

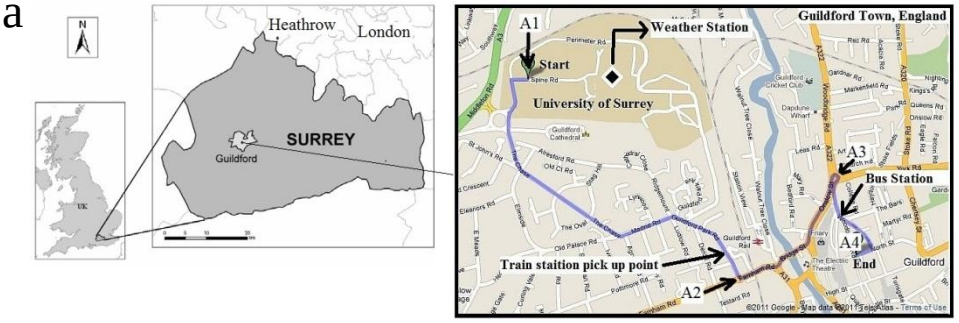

b

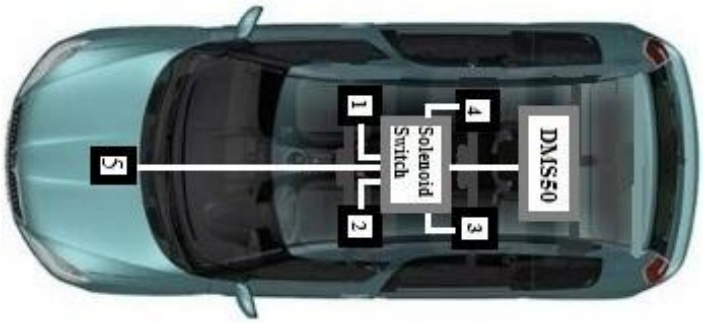

Figure 2 (Colour).pptx

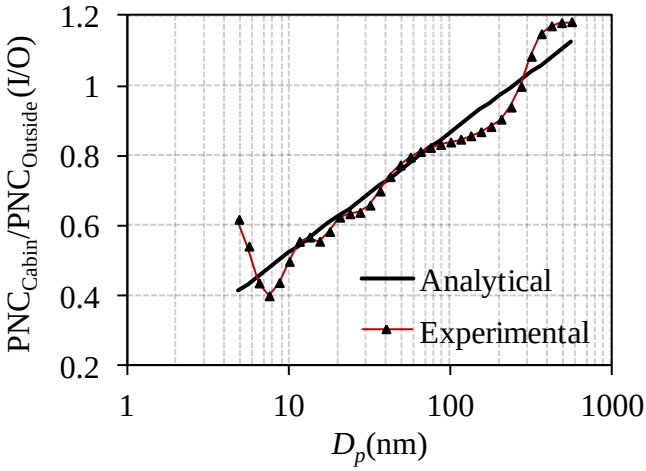

Figure 3 (Colour).pptx

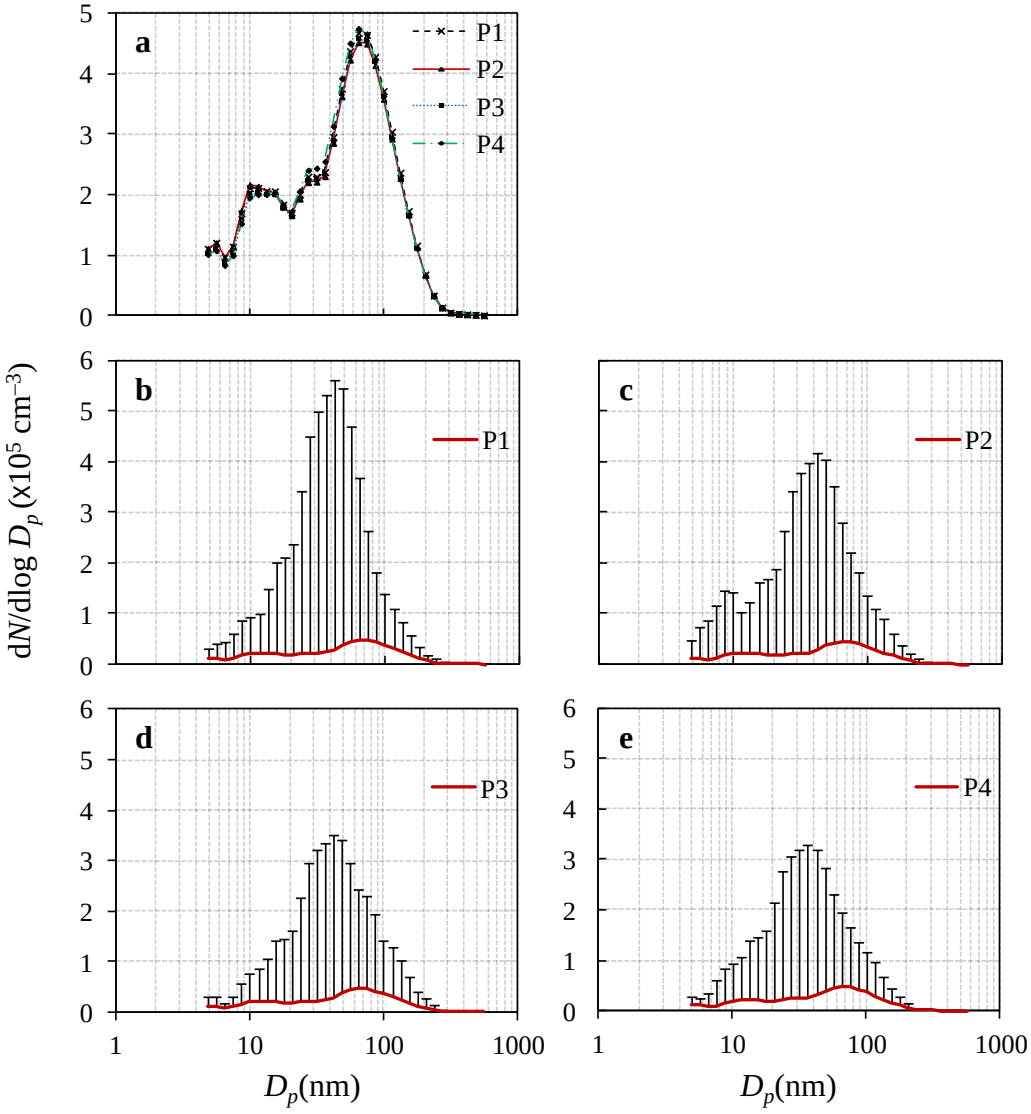

Figure 4 (Colour).pptx

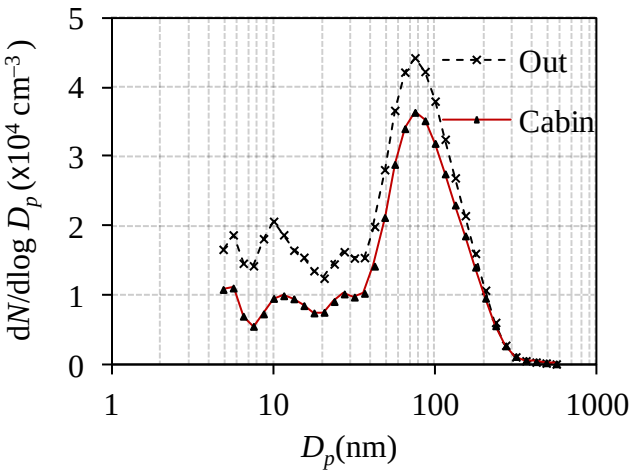

Figure 5 (Colour).pptx

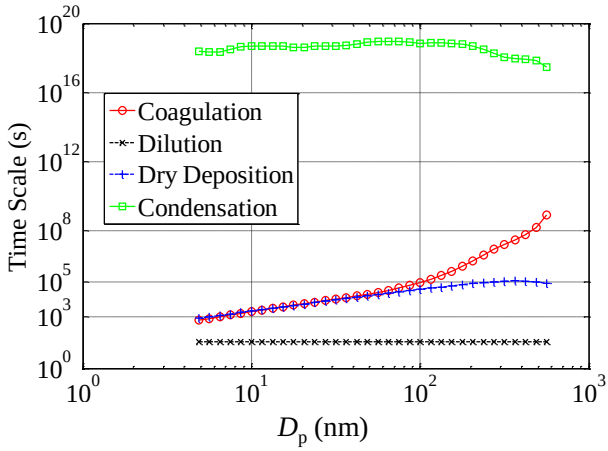

Figure 6 (Colour).pptx

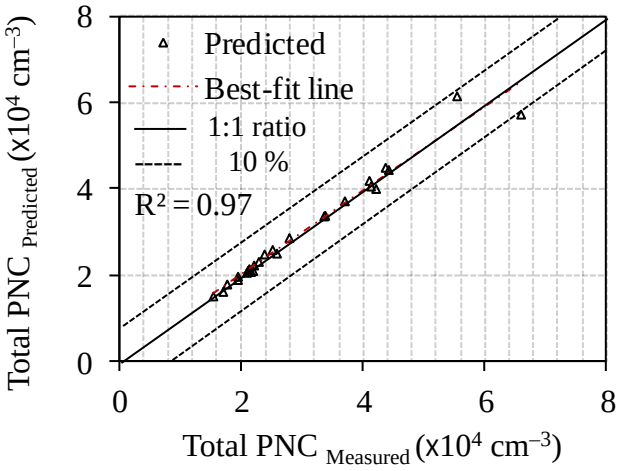

Figure 7 (Colour).pptx

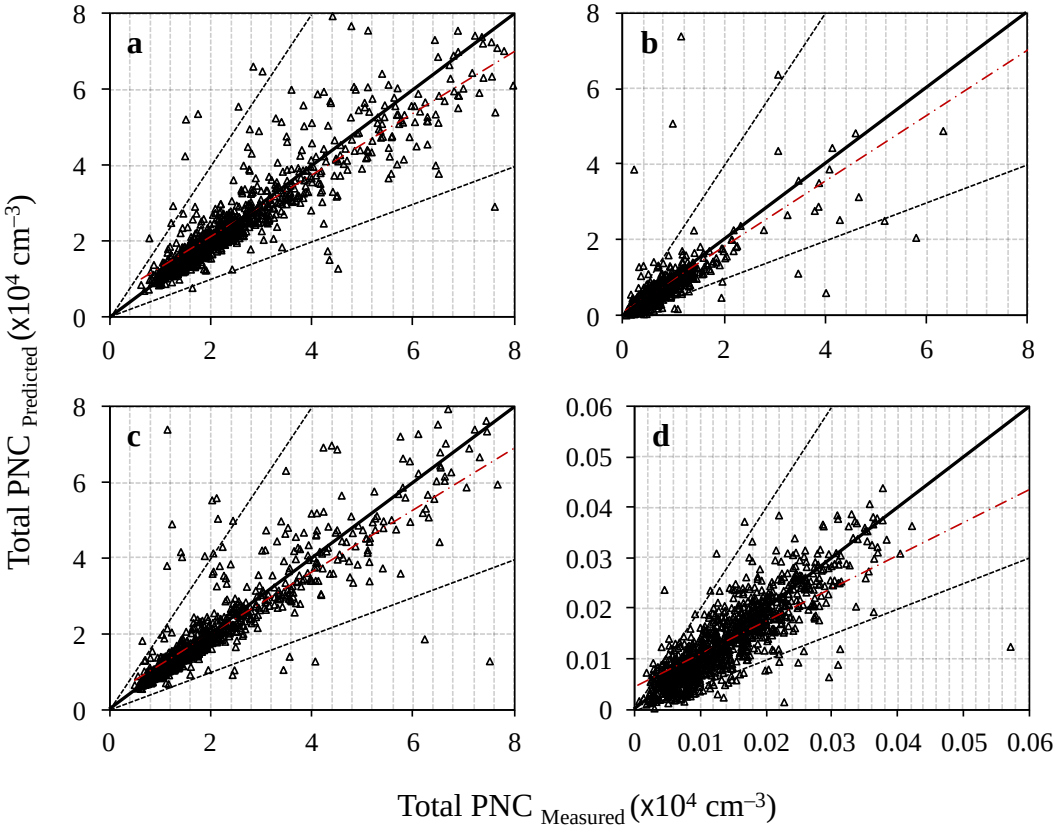

Figure 8 (Colour).pptx

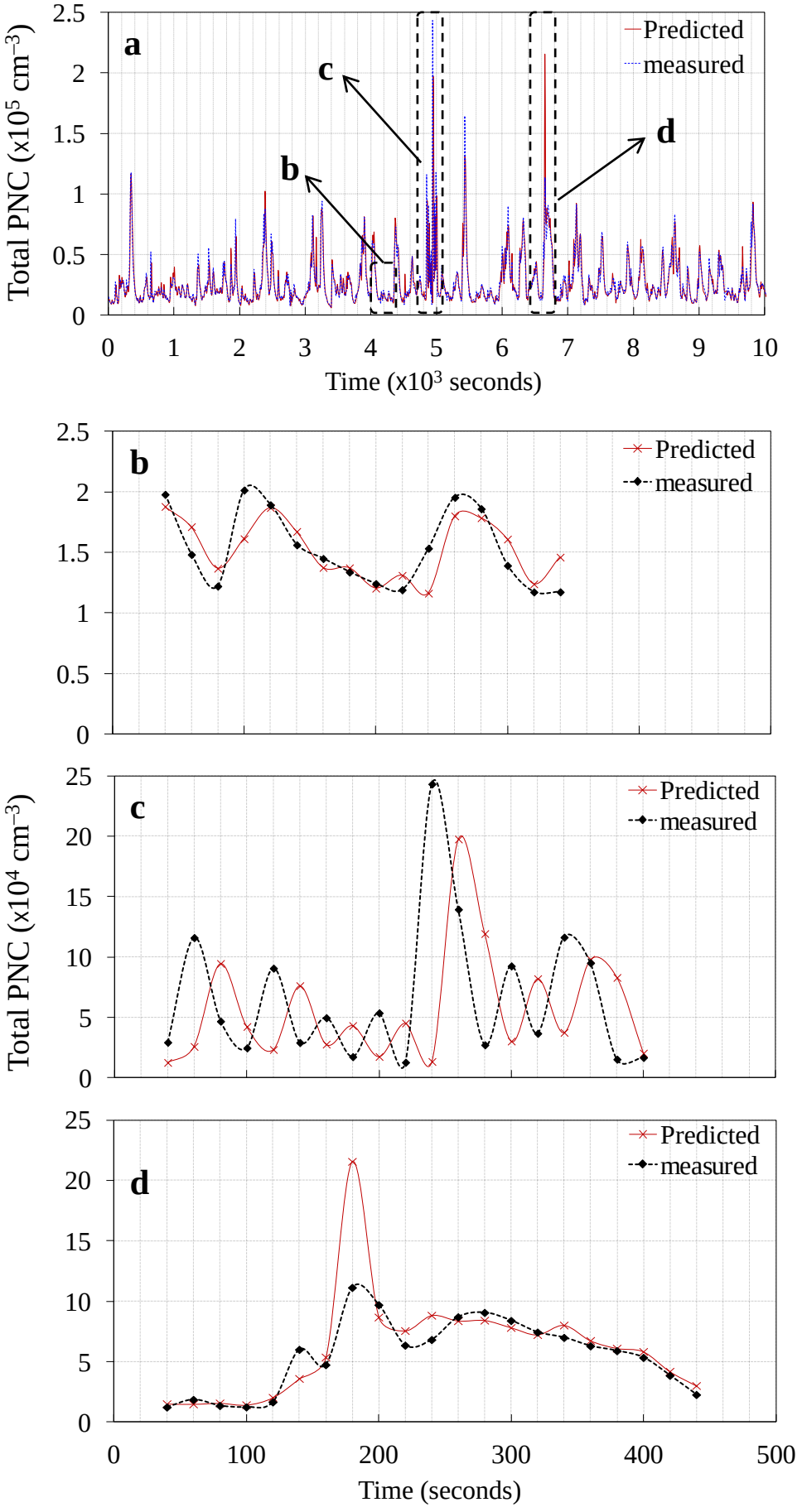

Figure 1 (B&W).pptx

a

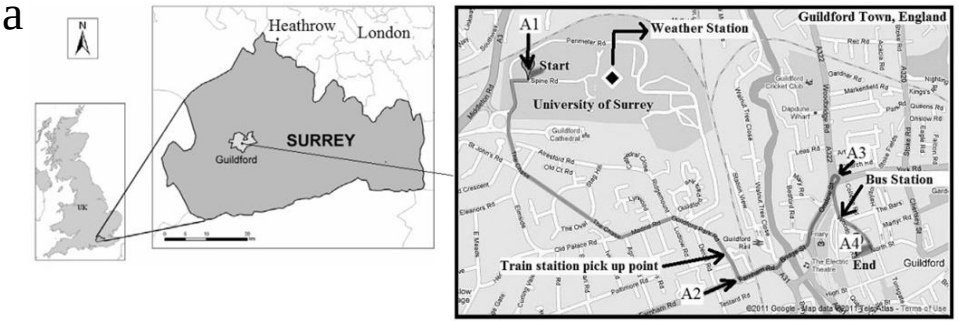

b

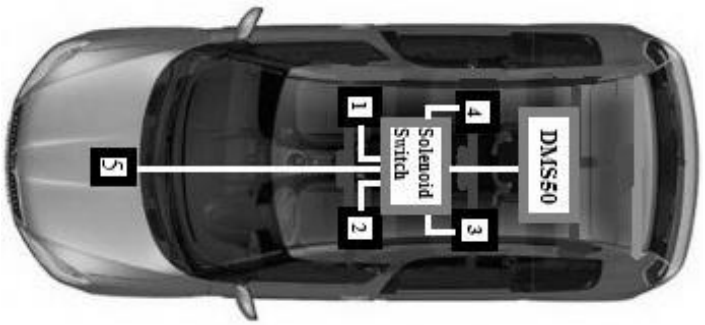

Figure 2 (B&W).pptx

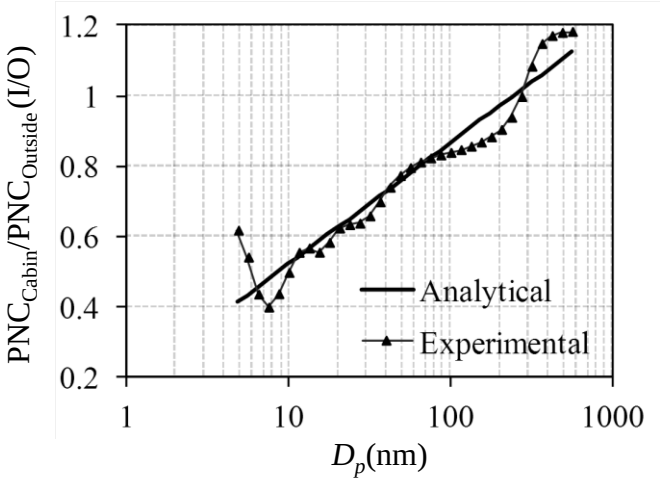

Figure 3 (B&W).pptx

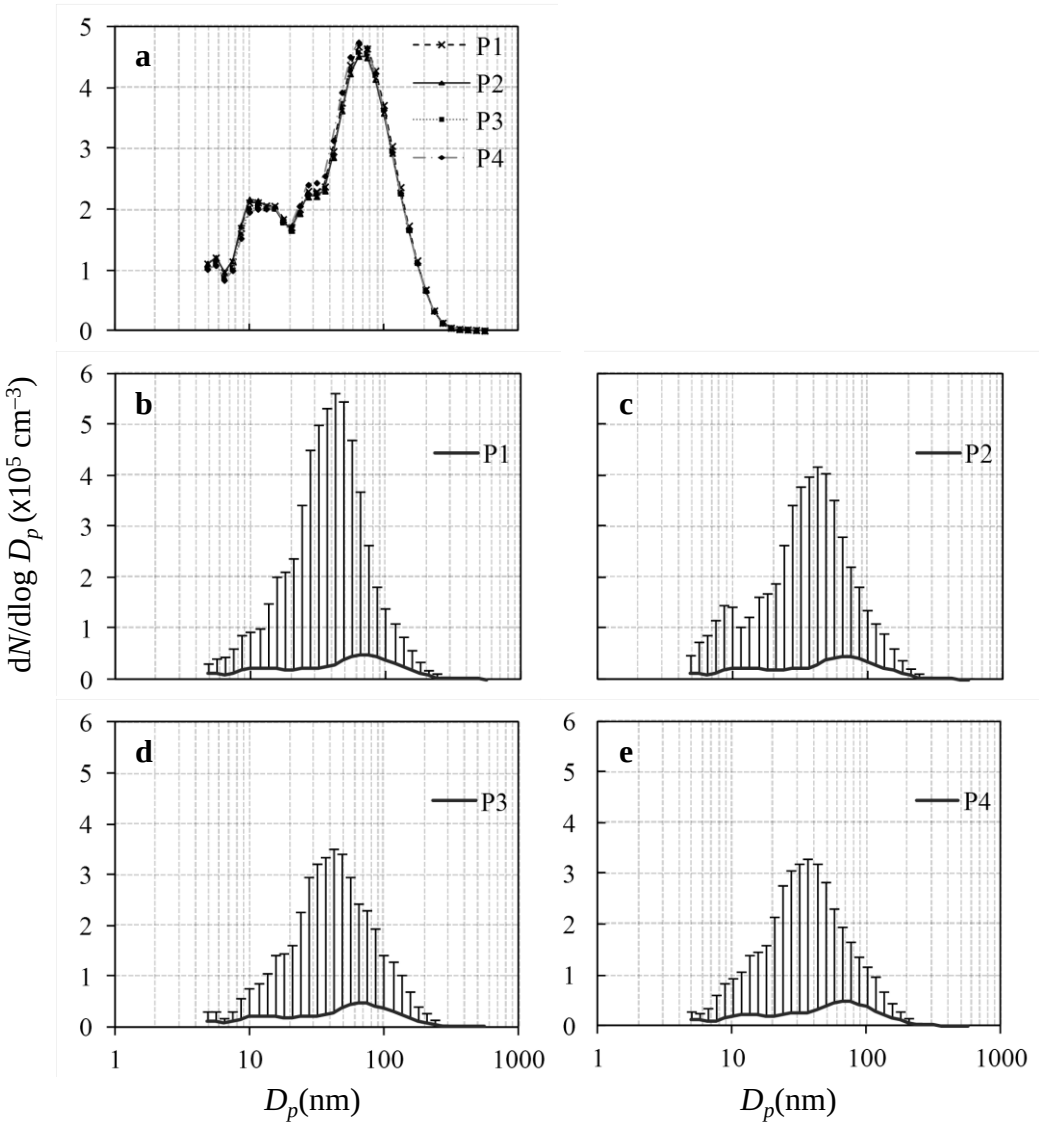

Figure 4 (B&W).pptx

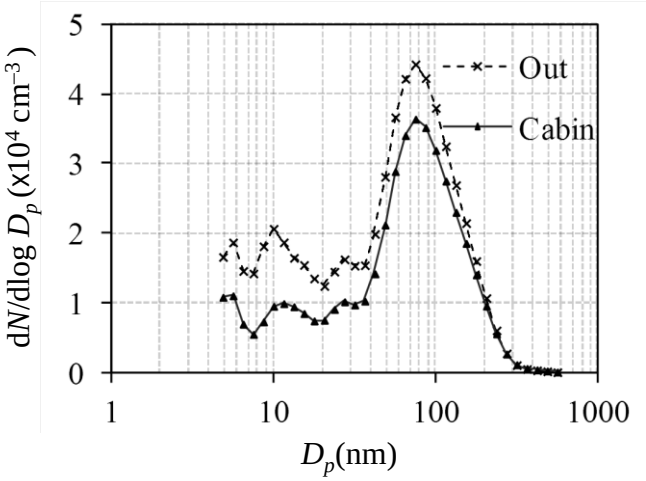

Figure 5 (B&W).pptx

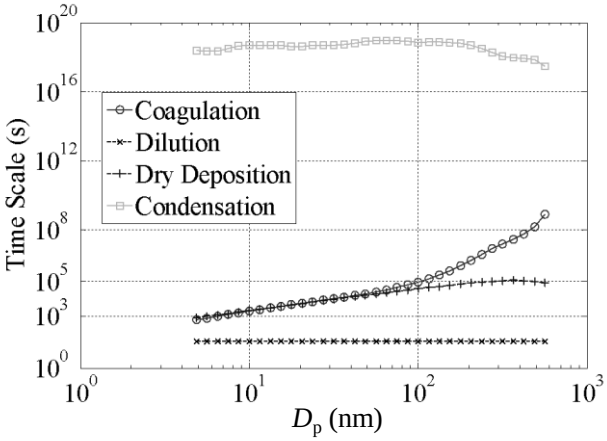

Figure 6 (B&W).pptx

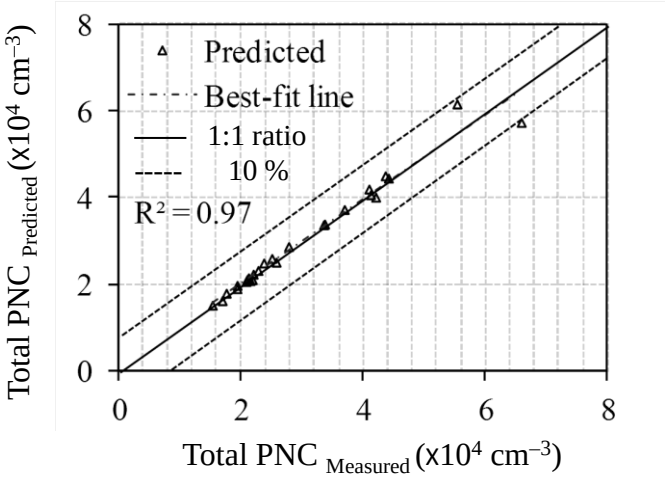

Figure 7 (B&W).pptx

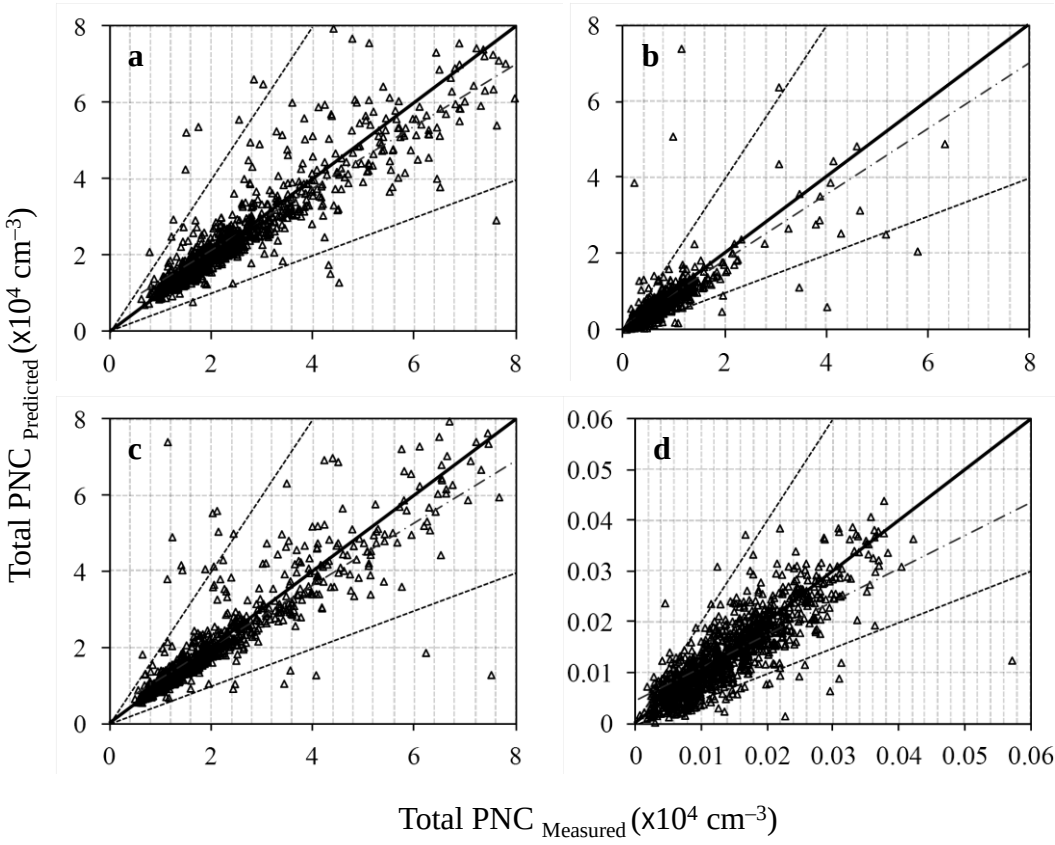

Figure 8 (B&W).pptx